Effect of halo modeling on weakly interacting massive particle exclusion limits

Anne M. Green
Physics Department, Stockholm University, Stockholm, S106 91, Sweden
(Received 18 July 2002; published 11 October 2002)

WIMP direct detection experiments are just reaching the sensitivity required to detect galactic dark matter in the form of neutralinos. Data from these experiments are usually analyzed under the simplifying assumption that the Milky Way halo is an isothermal sphere with Maxwellian velocity distribution. Observations and numerical simulations indicate that galaxy halos are in fact triaxial and anisotropic. Furthermore, in the cold dark matter paradigm galactic halos form via the merger of smaller subhalos, and at least some residual substructure survives. We examine the effect of halo modeling on WIMP exclusion limits, taking into account the detector response. Triaxial and anisotropic halo models, with parameters motivated by observations and numerical simulations, lead to significant changes which are different for different experiments, while if the local WIMP distribution is dominated by small scale clumps then the exclusion limits are changed dramatically.

DOI: 10.1103/PhysRevD.66.083003 PACS number(s): 98.70.Vc, 98.80.Cq

I. INTRODUCTION

Arguably the best motivated nonbaryonic dark matter candidate is the neutralino (the lightest supersymmetric particle), and current direct detection experiments are just reaching the sensitivity required to probe the relevant region of parameter space [1]. The most stringent exclusion limits on weakly interacting massive particles (WIMPs) in general currently come from the Edelweiss [2] and Cryogenic Dark Matter Search (CDMS) experiments [3], with competitive constraints also having been produced by Heidelberg-Moscow [4] and IGEX [5]. The sensitivity to WIMPs will be improved significantly in the short term future by the continued operation of Edelweiss, and CDMS moving in a low background environment at the Soudan mine [6], and in the longer term by, for instance, the planned GENIUS project [7].

The direct detection event rate, and its energy distribution, depend crucially on the WIMP speed distribution. Data analyzes nearly always assume a standard smooth halo model with isotropic Maxwellian velocity distribution. The change in the expected signal has been calculated for various nonstandard halo models of varying degrees of sophistication [8–11]. For models which are effectively close to Maxwellian, while there may be a significant change in the annual modulation and angular dependence of the signal, the change in the mean (averaged over time and recoil direction) differential event rate is typically small [8]. Models with triaxiality or velocity anisotropy may however produce a significant change even in the mean differential event rate [9,10]. Furthermore all of the nonstandard halo models which have previously been considered are essentially smooth.[1] *N*-body simulations, however, produce dark matter halos which as well as being triaxial with anisotropic velocity distributions [13,14] also contain substructure [15]. A number of groups have recently investigated the local dark matter distribution numerically [16,13,14], using different methods and reaching, to some extent, different conclusions.

Triaxiality, anisotropy and clumping in the WIMP velocity distribution could potentially have a significant effect on the WIMP direct detection signal. Constraints (and in the future possibly best fits) calculated assuming a standard Maxwellian halo could be erroneous [10]. On the other hand, more optimistically, it might be possible to derive useful information about the local velocity distribution, and hence the formation of the galactic halo, if WIMPs were detected [14,16]. Belli *et al.* [17] have recently reanalyzed the DAMA Collaborations annual modulation signal [18] for a range of halo models, finding that the allowed region of WIMP mass–cross-section parameter space is significantly enlarged. This illustrates that it is important to take into account uncertainties in halo modeling when comparing exclusion limits and/or allowed regions from different experiments.

Given the importance of the local dark matter distribution for direct detection experiments we devote Sec. II to a detailed discussion of the global properties of real and simulated dark matter halos and recent work on the local dark matter distribution [16,13,14]. In Sec. III we examine the effect of realistic halo modeling on exclusion limits. We first investigate triaxial and anisotropic halo models, with parameter choices motivated by the observations and simulations, and then, more speculatively examine the possible effects of small subhalos.

II. GALAXY HALOS

A. Global properties

Observational constraints on the structure of dark matter halos depend on the relation of luminous tracer populations to the underlying density distribution, and are complicated by galactic structure and projection effects. Reference [19] concludes that in the outskirts of spiral galaxies the intermediate-to-long axis ratio is likely to be greater than 0.8, while the short-to-long axis ratio is largely uncon-

[1]An exception is Sikivie's late infall model [12], which contrary to the standard picture of halo formation in cold dark matter (CDM) cosmologies (see, e.g., Refs. [13,14]) assumes axial symmetry and cold collapse.

strained with values in the range 0.3–1.0 reported, with some correlation between the method used and the value obtained (see Refs. [19] and [20] for details and references). For the Milky Way (MW), analysis of local stellar kinematics gives an estimate for the short-to-long axis value of 0.7 ± 0.1 [20], while the great circle tidal streams observed from the Sagittarius dwarf galaxy rule out ratios of less than 0.7 in the outer halo at high confidence [21] (in a flattened potential angular momentum is not conserved, so that orbits precess and tidal streams lose their coherence). The (an)isotropy of velocities in the MW halo is even harder to probe, however there is some evidence that galactic globular clusters may have preferentially radial orbits [22].

Given the difficulties involved in ''observing'' galaxy halos it makes sense to turn to numerical simulations for information on their possible structure. Current simulations of galaxy halos within a cosmological context can resolve subkpc scales (see e.g. [15,23]). Discrepancies between the halos produced in these simulations (which have lots of surviving dwarf galaxy sized subhalos and steep central profiles) and observations, have led to claims of a crisis for the cold dark matter model (see Ref. [24] and references therein for extensive discussion). Most relevant for the local dark matter distribution is the subhalo problem which may be, at least partly, due to complications in comparing the observed luminous matter with the dark matter distribution from the simulations. In particular it has been argued that gas accretion onto low mass halos may be inhibited after reionization so that a large fraction of the subhalos remain dark [25]. It has also been shown that if the observed dwarf galaxies themselves have dark halos, then their masses have been underestimated and correcting for this would go toward resolving the discrepancy with observations [26,27]. The survival of subhalos is at least partly due to their concentrated profiles, so any modification to the simulations which produced halos with shallower central profiles could also reduce the number of surviving subhalos. Despite the ongoing debate regarding the detailed comparison of the small scale properties of simulated halos with observations, cosmological simulations may still provide us with useful information about the global properties of dark halos.

The shape of simulated halos varies, not just between different halos of the same mass, but also as a function of radius within a single halo, strongly if the halo has undergone a major merger relatively recently. Two high resolution Local Group halos studied in detail in Ref. [13] have axis ratios of 1:0.78:0.48 and 1:0.45:0.38 at the solar radius and 1:0.64:0.40 and 1:0.87:0.67 at the virial radius. Adding dissipative gas to simulations tends to preserve the short-to-long axis ratio while increasing the intermediate-to-long axis ratio [28].

The anisotropy parameter $\beta(r)$, defined as

$$\beta(r) = 1 - \frac{\langle v_\theta^2 \rangle + \langle v_\phi^2 \rangle}{2\langle v_r^2 \rangle}, \tag{1}$$

where $\langle v_\theta^2 \rangle$, $\langle v_\phi^2 \rangle$ and $\langle v_r^2 \rangle$ are the means of the squares of the velocity components evaluated at radius r, also varies with radius. Typically $\beta(r)$ grows, although not monotonically, from roughly zero in the center of the halo to close to one at the virial radius, with non-negligible variation between halos (see Fig. 23 of Ref. [29]). The high resolution galactic mass halos studied in Ref. [30] have $\beta(R_\odot)$ in the range 0.1–0.4, corresponding to radially biased orbits.

B. Local dark matter distribution

In CDM cosmologies structure forms hierarchically, from the top down [31]. Small objects (often known as subhalos) form first, with larger objects being formed progressively via mergers and accretion. The internal structure of large galaxy size halos is determined by the dynamical processes which act on the accreted components. Dynamical friction causes subhalos with mass $M \gtrsim 10^9 M_\odot$ to spiral toward the center of their parent halo within a Hubble time [32], while the tidal field of the main halo can strip material away from a subhalo [32,26] producing tidal streams along its orbit [33].

The local dark matter distribution cannot be probed directly by cosmological simulations; the smallest subhalos resolvable in the highest resolution simulations have mass of order $10^7 M_\odot$ and it is not possible to fully resolve substructure within subhalos. Little substructure is found within the central regions of simulated halos, however it is not known whether the subhalos have been destroyed by tidal stripping or if this is purely a resolution effect [13]. This is crucial for the local dark matter distribution as the solar radius ($R_\odot \approx 8$ kpc) is small compared with the radius of the MW halo, which from observations is thought to be in excess of 100 kpc [19], while simulated halos with the same peak circular velocity as the MW have virial radii[2] of order 200 kpc. The computing power required to directly probe the local dark matter distribution will probably not be available for a decade or so [13], therefore other numerical [13,14] and semianalytic [16] approaches have been used to address the problem.

Stiff, Widrow and Frieman [16] employ a semianalytical approach, calculating the subhalo distribution as a function of mass and accretion redshift using the extended Press-Schechter formalism [35] and then evolving individual late accreting smooth subhalos within a growing spherical halo, to find the probability distribution of the overdensity at the solar radius. They find that there is a high (of order one) probability that there is a density enhancement of $\sim 3\%$ of the mean halo density in the solar neighborhood, and the probability of an enhancement roughly equal to the background density is non-negligible (of order 0.01).[3] They show that if the velocity of the clump, or stream, with respect to the Earth is high enough it will produce a shoulder in the differential event rate at high energies.

[2]The virial radius is the radius which separates the virialized and infall regions of simulated halos and has a mean density within it of 178 (100) times the critical density at $z=0$ in the standard (with cosmological constant) CDM cosmology [34].

[3]These probabilities are lower limits as they only include the contributions of subhalos accreted after $z=1$.

Moore *et al.* [13] take a region with dynamical properties similar to the local group, resimulated at higher resolution from a standard CDM cosmological simulation, and identify a subhalo with mass similar to the Draco dwarf galaxy. They then resimulate this subhalo up until its merger with the parent halo, at which point roughly 10% of its mass is in the form of (sub)subhalos. To assess the effect of tidal friction, subhalos with smooth density profiles are evolved within a smooth galactic potential and it is found that small subhalos orbiting at the solar radius which are accreted onto the galactic halo early retain most of their mass due to their high central densities.

Moore *et al.* conclude that the phase space distribution at the solar radius will depend crucially on the Galaxy's merger history and on the internal structure of the smallest subhalos, arguing that it is possible that the local dark matter density could be zero or that a single dark matter stream with small velocity dispersion could dominate or that many tidal streams could overlap to give a smooth distribution. The solution to this problem depends on the extent to which the substructure within subhalos is destroyed prior to their accretion onto the main halo. The subhalos are of course also formed hierarchically themselves from smaller subhalos. The free-streaming length of neutalinos is so small that the first clumps to form have mass $M \sim 10^{-12} M_{\odot}$ [36], however, and to follow the accretion and destruction of subhalos though such a large hierarchy of scales would be decidedly nontrivial.

Helmi, White and Springel [14] take a cosmological ΛCDM simulation, where the second largest cluster has been resimulated at higher resolution and then scaled down in size to match the MW. Most of the mass in the inner halo has been in place for 10 Gyr and the smallest resolvable subhalos do not survive to the present day at the solar radius. They argue that the only way a small subhalo with high density could exist in the solar neighborhood at $z=0$ is if it were first accreted by a large halo which subsequently had a major merger with the main progenitor of the galactic halo. They conclude that the local dark matter velocity distribution is well approximated by a smooth multivariate Gaussian, with clumps of high velocity particles present if the MW halo has undergone a recent major merger.

In summary, numerical simulations produce galaxy halos which are significantly triaxial and anisotropic, with the shape and anisotropy of a halo depending on its individual merger history, a picture which is broadly supported by observations. This indicates that, even if the local velocity distribution is relatively smooth, the standard spherical isotropic Maxwellian halo model may not be a good approximation. Furthermore, galaxy halos are formed hierarchically from the accretion of smaller subhalos, which may not be completely destroyed by tidal friction, so that the local dark matter could be distinctly nonsmooth. It is even possible that the dark matter could be distributed largely in small dense clumps. There is currently no consensus on the local dark matter velocity distribution however, with the results obtained depending on the method used to extrapolate to small scales below the resolution limit of cosmological simulations, so this possibility should be regarded as speculative.

III. EFFECTS ON EXPERIMENTAL ANALYSIS

The differential WIMP event rate due to scalar interactions can be written in terms of the WIMP scattering cross section on the proton, $\sigma_{\rm p}$ [37]:

$$\frac{dR}{dE} = \zeta \sigma_{\rm p} \left[\frac{\rho_{0.3}}{\sqrt{\pi} v_0} \frac{(m_{\rm p}+m_\chi)^2}{m_{\rm p}^2 m_\chi^3} A^2 T(E) F^2(q) \right], \qquad (2)$$

where the local WIMP density ρ_χ is normalized to a fiducial value $\rho_{0.3}=0.3$ GeV/ cm^3, such that $\zeta=\rho_\chi/\rho_{0.3}$, m_A is the atomic mass of the target nuclei, E is the recoil energy of the detector nucleus, and $T(E)$ is defined as [37]

$$T(E) = \frac{\sqrt{\pi} v_0}{2} \int_{v_{\rm min}}^{\infty} \frac{f_v}{v} dv, \qquad (3)$$

where f_v is the WIMP speed distribution in the rest frame of the detector, normalized to unity, and $v_{\rm min}$ is the minimum detectable WIMP speed

$$v_{\rm min} = \left(\frac{E(m_\chi+m_A)^2}{2 m_\chi^2 m_A} \right)^{1/2}. \qquad (4)$$

A. Triaxiality and anisotropy

We will first examine the change in the WIMP speed distribution for triaxial and anisotropic, but still smooth, halo models. To date two self-consistent triaxial and/or anisotropic halo models have been studied in relation to WIMP direct detection: the logarithmic ellipsoidal model [9] and the Osipkov-Merritt anisotropy model [38], studied in Ref. [10]. We will extend the previous work by focusing on parameters which span the range of halo properties discussed in Sec. II above and including the detector response.

The logarithmic ellipsoidal model [9] is the simplest triaxial generalization of the isothermal sphere and the velocity distribution can be approximated by a multivariate gaussian on either the long or the intermediate axis (see Appendix A for further details).[4] We consider parameter values $p=0.9$,$q=0.8$ corresponding to axial ratios 1:0.78:0.48 (as used in Ref. [9]), and $p=0.72$,$q=0.70$ corresponding to 1:0.45:0.38, and locations on the long and intermediate axes. The first set of axial ratios is typical of the values found in simulations and roughly consistent with observations, while the second is arguably rather extreme. We use values of the anisotropy parameter γ (which in the spherical limit $p=q=1$ is related to β by $-\gamma=2\beta$) which give $\beta=0.1$ and 0.4, and are tabulated in Table I. The speed distributions, in the rest frame of the Sun normalized to unity, are plotted in Fig. 1 along with that for the standard Maxwellian halo model. For both positions the triaxial models have a wider spread in speeds than the standard model, so that the differential event rate will decrease less rapidly with increasing recoil energy, but the change is small on the major axis. This is because the change

[4]Of course there is no reason to expect the Sun to be located on one of the axes of the halo.

TABLE I. The values of the anisotropy parameter γ in the logarithmic ellipsoidal model required to produce $\beta=0.1$ and 0.4.

β	$p=0.9$, $q=0.8$	$p=0.72$, $q=0.7$
	intermediate axis	
0.1	0.07	4.02
0.4	−0.62	2.01
	major axis	
0.1	−1.00	−1.39
0.4	−1.33	−1.60

in the speed distribution is largely determined by the velocity dispersion in the ϕ direction. On the major axis, for parameter values which give $0.1<\beta<0.4$, all three components of the velocity have roughly the same dispersion, whereas on the intermediate axis the velocity dispersion in the ϕ direction is significantly larger than that in the z direction. Note that the speed distributions we consider deviate less from the standard Maxwellian than those considered by Refs. [9] and [17] as they use more extreme values for γ (namely 16 and -1.78).

In the Osipkov-Merritt (OM) model (see Appendix B for further details), which assumes a spherically symmetric density profile, the velocity anisotropy varies as a function of radius as

$$\beta(r)=\frac{r^2}{r^2+r_a^2}, \tag{5}$$

so that the degree of anisotropy increases with increasing radius, as is found in numerical simulations. Following Ref. [10] we assume a Navarro-Frenk-White (NFW) [39] density profile[5] with scale radius $r_s=20$ kpc. We use values of the anisotropy radius $r_a=20,12$, and 9.8 kpc which correspond to $\beta(R_0)=0.14,0.31$ and 0.4, respectively. For the first two values analytic fitting functions for the distribution function have been provided by Widrow [40]. The resulting speed distributions are plotted in Fig. 2 along with that for the standard Maxwellian halo model. The excess at large v is due to the increased number of particles on very elongated, nearly radial orbits [10].

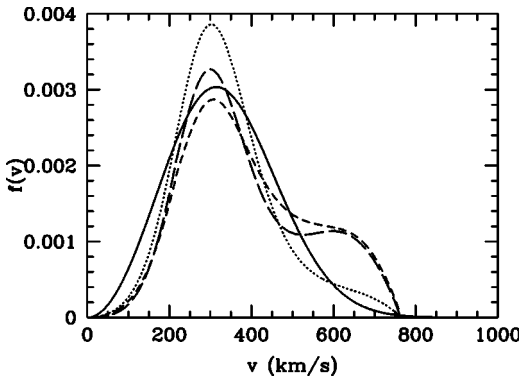

FIG. 2. The speed distributions for the standard halo model (solid line), and the OM anisotropy model with $\beta=0.13$, 0.31 and 0.4 (dotted, short-dashed, and long-dashed).

To assess the effect of changes in the speed distribution on exclusion limits we need to take into account the detector response, including the difference between the observed energy of an event and the actual recoil energy, nonzero energy threshold and energy resolution (see Ref. [41] for further details), as these factors may blur out the effects of changes in the speed distribution. We consider a Ge^{76} detector with energy threshold $E_T=4$ keV with the same properties (resolution and form factor) as that used by the IGEX experiment [5], which is optimized for detecting double-beta decay. The resulting differential event rates, per kg per day per keV, are plotted in Fig. 3, for the OM speed distributions in Fig. 2, for WIMPs with mass $m_\chi=50$ GeV and cross section $\sigma_p=10^{-45}$ m^2. We see that, in this model, the differential event rate does not deviate linearly from that of the standard halo model as the degree of anisotropy is increased. Since future detectors, optimized for WIMP detection, will have lower thresholds and better energy resolution, we also plot the dif-

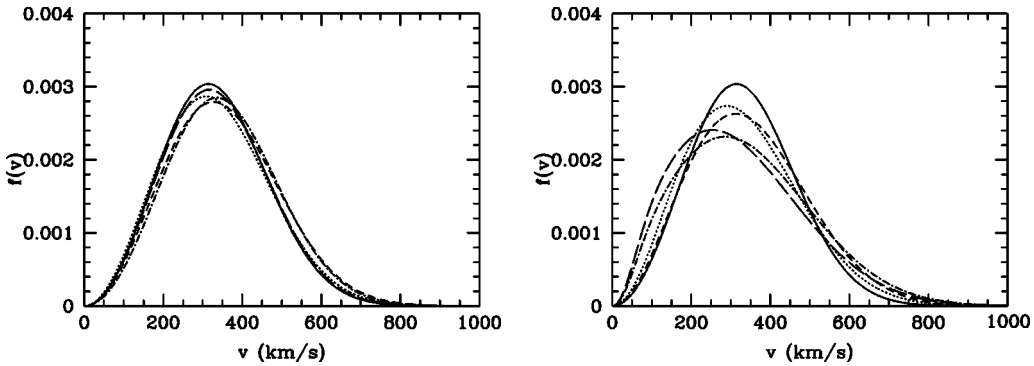

FIG. 1. The speed distributions, in the rest frame of the Sun, for the standard halo model (solid line), and triaxial models on the major axis (upper panel) and intermediate axis (lower panel) for $p=0.9$, $q=0.8$ and $\beta=0.1/0.4$ (dotted and short dashed) and for $p=0.72$, $q=0.7$ and $\beta=0.1/0.4$ (long dashed and dot dashed).

[5]Varying the inner slope of the density profile does not significantly affect the local velocity distribution [10].

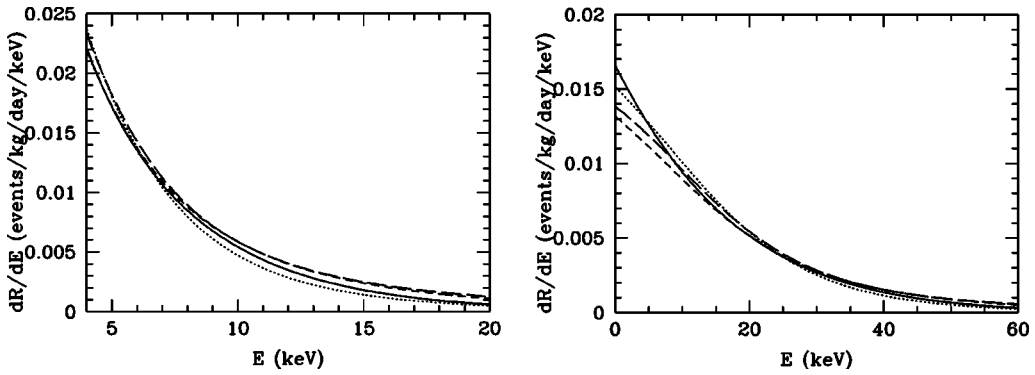

FIG. 3. The differential event rate for the OM anisotropy model, with speed distributions as plotted in Fig. 2, for $m_\chi = 50$ GeV and $\sigma_p = 10^{-45}$ m^2 for the IGEX detector (upper panel) and for an "ideal" Ge detector (lower panel).

ferential event rates for an "ideal" (i.e., completely unrealistic) $A = 76$ detector where the full recoil energy is detected, the energy resolution is perfect and $E_T = 0$ keV.[6] The difference between the differential event rates is then largest at small recoil energies, and would therefore be more significant for an experiment with a lower threshold energy.

In Fig. 4 we plot the exclusion limits found from the IGEX data by requiring that the data in no more than one energy bin exceed its 99.77% confidence limit, so as to produce 90% overall confidence limits [42], for the logarithmic ellipsoidal model and for the OM anisotropy model. We also plot the exclusion limits from the Heidelberg-Moscow (HM) experiment [4] for the OM anisotropy model in Fig. 5. Comparing Figs. 4 and 5 we see that the change in the exclusion limits depends not only on the halo model under consideration, but also on the data being used; for IGEX the change in the exclusion limits is largest for large WIMP masses, while for HM the change is largest for small WIMP masses. For different WIMP masses, different energy ranges can be most constraining; for the IGEX data the lowest energy bin is always the most constraining, while for HM as the WIMP mass increases the constraint comes from higher energy bins. It should therefore be borne in mind when comparing exclusion limits from different experiments, that changing the assumed WIMP speed distribution will affect the limits from different experiments differently.

The change in the exclusion limits is not huge (of order tens of percent) for the experiments we have considered; however, these experiments are not optimized for WIMP detection. As illustrated in Fig. 3 the change in the differential event rate, and hence the exclusion limit, would be significantly larger for an experiment with better energy resolution and lower threshold energy. We have also seen that different models with the same value for the anisotropy parameter β have very different speed distributions, and hence a different effect on the exclusion limits. Furthermore it is conceivable that the local WIMP velocity distribution may deviate even further from the standard Maxwellian distribution than the models that we have considered.

B. Clumps

Even if dynamical processes produce a smooth background dark matter distribution, late accreting clumps may lead to a local density enhancement and velocity clumping [14,16], and produce a shoulder in the differential event rate,

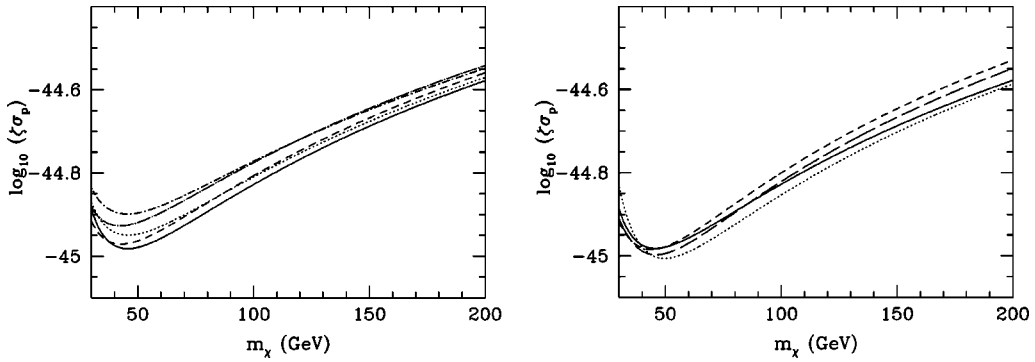

FIG. 4. The exclusion limits from the IGEX experiment for the logarithmic ellipsoidal model, located on the intermediate axis (upper panel) and for the OM model (lower panel). Line types as in the lower panel of Fig. 1 and Fig. 2, respectively.

[6]Somewhat counterintuitively, at low energies the differential event rate for the IGEX detector is higher than that for the ideal detector, due to the finite energy resolution of the IGEX detector.

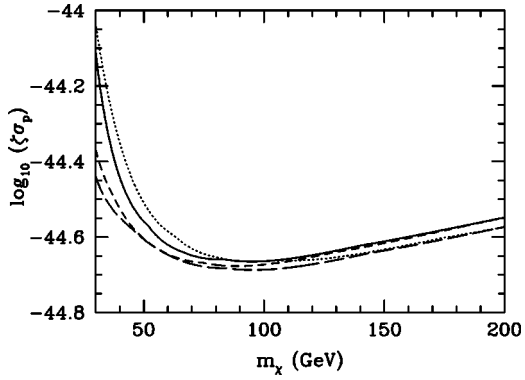

FIG. 5. The exclusion limits from the HM experiment for the OM model. Lines as in Fig. 2.

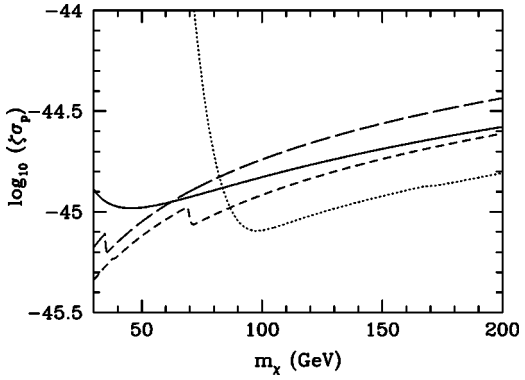

FIG. 6. The exclusion limits from the IGEX data if a subhalo with negligible velocity distribution moving with speed 200, 400, 600 kms^{-1} relative to the earth (dotted, short dashed, long dashed) dominates the local density.

if their density and velocity with respect to the Earth are large enough. For the experiments we have been considering the lower energy bins are most constraining, so that only very rare high density and velocity streams would have a non-negligible effect on the exclusion limits. The effect of these late accreting clumps on the annual modulation and directional signals would be more significant however [16].

We will now turn our attention to the consequences of the more speculative possibility that small subhalos may survive at the solar radius. We could then be located within a subhalo with local density in excess of the mean value of 0.3 GeV cm^{-3}, on the other hand it is even possible that we could be in a region between clumps and streams where the WIMP density is zero [13]. In the latter case all attempts at WIMP direct detection would be doomed to failure, and exclusion limits would tell us nothing about the WIMP cross section. At the other extreme a tiny subhalo at the Earth's location would produce a distinctive signal and, due to the enhanced density, make it easier to detect WIMPs of a given cross section. Subhalos with $M \ll 10^9 M_\odot$ would have negligible velocity dispersion and hence a delta-function speed distribution. The resulting theoretical differential event rate would be a step function with amplitude inversely proportional to the speed of the subhalo with respect to the Earth, and position increasing with increasing relative speed and WIMP mass. Consequently for small subhalo velocities and WIMP masses there would be no constraint on the WIMP cross section (no WIMPs would have sufficient energy to cause an observable recoil), but as the WIMP mass is increased the constraints would become much tighter as then all the WIMPs would be energetic enough to cause events of a given recoil energy. In Fig. 6 we plot the exclusion limits on $\zeta\sigma_p$ from the IGEX data for subhalos with various relative speeds[7] dominating the local WIMP distribution. Unlike the smooth halo models for this data set, as the WIMP mass is increased higher energy bins are most constraining, and this leads to sharp changes in the exclusion limits due to the sharp transition from no WIMPs to all WIMPs having sufficient energy to cause events of a given recoil energy. Note that the high density of a subhalo would lead to $\xi > 1$, so that the exclusion limits on the WIMP cross section would be tighter (by some unknown factor) than for the standard halo model.

How dense could small scale clumps be? Dark matter clump densities are usually parametrized in terms of their concentration, c, defined as

$$c = \frac{R_{\mathrm{vir}}}{r_s}, \tag{6}$$

where R_{vir} is the virial radius and r_s is the scale radius, the radius at which the effective logarithmic slope of the density profile is equal to -2 (see e.g. Refs. [43,44]). Low mass halos typically form earlier, when the density of the Universe is higher, so that their concentrations are higher than those of larger halos [39] and Bullock *et al.* [43] and Eke, Navarro and Steinmetz (ENS) [44] have recently constructed toy models which reproduce the scaling of concentration with mass and redshift for the simulated galaxy-sized halos.

Since the first neutralino clumps to form have mass of order $10^{-12} M_\odot$ [36], the first generation of halos which are formed in the same way as galaxy sized halos (via the accretion and merger of smaller clumps) will have mass of order $10^{-10} M_\odot$, and virial radii of order 0.01 pc. While these clumps are tiny by cosmological standards, they are still relatively large compared to the distance traveled by the Sun in a year (10^{-4} pc). Extrapolating the Bullock *et al.* and ENS toy models way beyond their intended range of applicability produces significantly different ''guesstimates'' for c for $M \sim 10^{-10} M_\odot$ halos of 150 and 30, respectively [45]. Subhalos within larger halos may in fact be more concentrated than isolated halos of the same mass as dense regions tend to collapse earlier and tidal stripping may steepen their density profiles [43]. The tidal radius [32] of a $10^{-10} M_\odot$ subhalo orbiting in the MW halo at the solar radius is of order 10^{-3} pc, so the dense central regions of these subhalos should survive tidal stripping [13,26]. The density of simulated halos diverges toward their center, so as a measure of

[7]In reality the subhalo speed would be another unknown variable.

the typical density of a subhalo we use the mean density within the scale radius, assuming a NFW density profile [39]:

$$\rho(r) \propto \frac{r_s}{r(1+r/r_s)^2}. \tag{7}$$

For $c=30(150)$ this gives $\rho=0.9(70)$ GeV cm^{-3}, or equivalently $\zeta=3(200)$. We emphasize that this rough calculation relies on the extrapolation of the concentration-mass scaling models far beyond the regime in which they have been numerically tested (isolated galaxy mass halos) and the numbers obtained should probably not be taken seriously. It does illustrate, however, that *if* small subhalos survive then they *may* lead to a significant local enhancement in the WIMP density, and that understanding the small scale structure of galactic halos is crucial for realistic modeling of the WIMP velocity distribution.

IV. DISCUSSION

Rapid progress is being made in the field of WIMP direct detection, with experiments closing in on the sensitivity required to detect neutralinos, if they constitute a non-negligible fraction (greater than 10^{-4}) of the halo density [46]. Data analyses usually assume the simplest halo model: an isothermal sphere with Maxwellian velocity distribution. There is no clear justification, either observational or theoretical, for this assumption apart from simplicity. In fact numerical simulations [13–15] and observations [19,20,22] suggest that galaxy halos are triaxial and anisotropic. The local density distribution may also be non-smooth, with late accreting subhalos leading to velocity clumping [14,16]. More speculatively it is even possible that the dark matter could be mainly distributed in tiny dense clumps, so that the local density distribution could be dominated by a single clump, or could even be zero [13]. It is therefore crucial to examine the effect of realistic halo modeling on the WIMP direct detection signal.

In this paper we have investigated the change in exclusion limits due to triaxiality, velocity anisotropy and small scale clumping, taking into account detector performance and using parameter values motivated by numerical simulations and observations. Triaxiality and velocity anisotropy lead to non-negligible changes in the exclusion limits, even for detectors with relatively poor energy resolution. Furthermore, the changes are different for different data sets and depend on how the anisotropy is modeled. If the local WIMP distribution is dominated by small scale clumps then the local density may be zero (making it impossible to detect WIMPs) or significantly enhanced (making it easier to detect WIMPs with a given cross section), and the exclusion limits are changed dramatically. Clearly the survival of subhalos at the solar radius is a very important issue for WIMP direct detection.

Even if the local WIMP distribution is smooth, to derive reliable constraints on WIMP parameters and compare results for different experiments a framework needs to be developed for dealing with the uncertainty in the WIMP velocity distribution: either the development of a framework for parametrizing deviations from a baseline model, or the establishment of an agreed set of benchmark models, spanning the range of plausible WIMP velocity distributions.

ACKNOWLEDGMENTS

A.M.G. was supported by the Swedish Research Council and would like to thank Amina Helmi and Ben Moore for answering questions about their work.

APPENDIX A: LOGARITHMIC ELLIPSOIDAL MODEL

The logarithmic ellipsoidal model [9] is the simplest triaxial generalization of the isothermal sphere and the velocity distribution can be approximated by a multivariate Gaussian on either the long or the intermediate axis:

$$f(v)=\frac{1}{(2\pi)^{3/2}\sigma_r\sigma_\phi\sigma_z}\exp\left(-\frac{v_r^2}{\sigma_r^2}-\frac{v_\phi^2}{\sigma_\phi^2}-\frac{v_z^2}{\sigma_z^2}\right). \tag{A1}$$

On the intermediate axis

$$\sigma_r^2=\frac{v_0^2 p^{-4}}{(2+\gamma)(1-p^{-2}+q^{-2})},$$

$$\sigma_\phi^2=\frac{v_0^2(2q^{-2}-p^{-2})}{2(1-p^{-2}+q^{-2})},$$

$$\sigma_z^2=\frac{v_0^2(2-p^{-2})}{2(1-p^{-2}+q^{-2})}, \tag{A2}$$

and on the major axis

$$\sigma_r^2=\frac{v_0^2}{(2+\gamma)(p^{-2}+q^{-2}-1)},$$

$$\sigma_\phi^2=\frac{v_0^2(2q^{-2}-1)}{2(p^{-2}+q^{-2}-1)},$$

$$\sigma_z^2=\frac{v_0^2(2p^{-2}-1)}{2(p^{-2}+q^{-2}-1)}, \tag{A3}$$

where p and q are constants which satisfy $q^2 \leqslant p^2 \leqslant 1$ and are related to the axial ratios of the density distribution, $I_{1,2}$, by

$$I_1^2=\frac{p^2(p^2q^2+p^2-q^2)}{q^2+p^2-p^2q^2},$$

$$I_2^2=\frac{q^2(p^2q^2-p^2+q^2)}{q^2+p^2-p^2q^2}, \tag{A4}$$

and γ is a constant isotropy parameter, which in the spherical limit $p=q=1$ is related to β [as defined in Eq. (1)] by $-\gamma=2\beta$.

APPENDIX B: OSIPKOV-MERRITT MODEL

The distribution function of a self-gravitating system with spherically symmetric density profile $\rho(r)$ is given, assuming an isotropic velocity distribution, by Eddington's formula [32] (see also Refs. [40,10]):

$$f(\varepsilon)=\frac{1}{\sqrt{8}\pi^2}\left[\int_0^{\varepsilon}\frac{d^2\rho}{d\Psi^2}\frac{d\Psi}{\sqrt{\varepsilon-\Psi}}+\frac{1}{\sqrt{\varepsilon}}\left(\frac{d\rho}{d\Psi}\right)_{\Psi=0}\right], \tag{B1}$$

where $\Psi(r)=-\Phi(r)+\Phi(r=\infty)$, $\Phi(r)$ is the potential of the system, $\varepsilon=-E+\Phi(r=\infty)=-E_{\rm kin}+\Psi(r)$, and E and $E_{\rm kin}$ are the total and kinetic energy, respectively. In the Osipkov-Merritt model [38] the distribution function also depends on the angular momentum, L, of the system through the variable $\mathcal{Q}$:

$$\mathcal{Q}\equiv\varepsilon-\frac{L^2}{2r_{\rm a}^2}, \tag{B2}$$

where $r_{\rm a}$ is the anisotropy radius, which is related to β by

$$\beta(r)=\frac{r^2}{r^2+r_{\rm a}^2}, \tag{B3}$$

so that the degree of anisotropy increases with increasing radius. The distribution function in the Osipkov-Merritt model is found by replacing ε by $\mathcal{Q}$ and $\rho(r)$ by $(1+r^2/r_{\rm a}^2)\rho(r)$ in Eq. (B1), which then has to be solved numerically. Analytic fitting functions have been provided by Widrow [40] for selected values of $r_{\rm a}$, for the NFW density profile [39]. Note that physical models only exist for $r_{\rm a}>r_{\rm a,min}$, where $r_{\rm a,min}$ depends on the potential.

[1] L. Bergström, Rep. Prog. Phys. **63**, 793 (2000).
[2] A. Benoit *et al.*, astro-ph/0206271.
[3] R. Abusaidi *et al.*, Phys. Rev. Lett. **84**, 5699 (2000); D. Abrams *et al.*, astro-ph/0203500.
[4] L. Baudis *et al.*, Phys. Rev. D **59**, 022001 (1999).
[5] A. Morales *et al.*, Phys. Lett. B **532**, 8 (2002).
[6] R. Schnee, in *Proceedings of "COSMO 2000,"* 4th International Workshop on Particle Physics and the Early Universe, edited by J. E. Kim, P. Ko, and K. Lee (World Scientific, Singapore, 2002), p. 99.
[7] L. Baudis *et al.*, in ''Sources and detection of dark matter in the universe,'' astro-ph/0005568.
[8] A.K. Drukier, K. Freese, and D.N. Spergel, Phys. Rev. D **33**, 3495 (1986); F. Donato, N. Fornengo, and S. Scopel, Astropart. Phys. **9**, 247 (1998); M. Kamionkowski and A. Kinkhabwala, Phys. Rev. D **57**, 3256 (1998); C.J. Copi, J. Heo, and L.M. Krauss, Phys. Lett. B **461**, 43 (1999); M. Brhlik and L. Roskzkowski, *ibid.* **464**, 303 (1999); J.D. Vergados, Phys. Rev. Lett. **83**, 3597 (1999); Phys. Rev. D **62**, 023519 (2000); P. Belli *et al.*, *ibid.* **61**, 023512 (2000); A.M. Green, *ibid.* **63**, 043005 (2001); C.J. Copi and L.M. Krauss, *ibid.* **63**, 043507 (2001); J.D. Vergados and D. Owen, astro-ph/0203293.
[9] N.W. Evans, C.M. Carollo, and P.T. de Zeeuw, Mon. Not. R. Astron. Soc. **318**, 1131 (2000).
[10] P. Ullio and M. Kamionkowski, J. High Energy Phys. **03**, 049 (2001).
[11] J.D. Vergados, Phys. Rev. D **63**, 063511 (2001); A.M. Green, *ibid.* **63**, 103003 (2001); G. Gelmini and P. Gondolo, *ibid.* **64**, 023504 (2001).
[12] P. Sikivie, I.I. Tkachev, and Y. Wang, Phys. Rev. Lett. **75**, 2911 (1995); Phys. Rev. D **56**, 1863 (1997); P. Sikivie, Phys. Lett. B **432**, 139 (1998).
[13] B. Moore *et al.*, Phys. Rev. D **64**, 063508 (2001).
[14] A. Helmi, S. D. M. White, and V. Springel, Phys. Rev. D **66**, 063502 (2002).
[15] A. Klypin *et al.*, Astrophys. J. **522**, 82 (1999); B. Moore *et al.*, Mon. Not. R. Astron. Soc. **310**, 1147 (1999).
[16] D. Stiff, L.M. Widrow, and J. Frieman, Phys. Rev. D **64**, 083516 (2001).
[17] P. Belli, R. Cerulli, N. Forengo, and S. Scopel, Phys. Rev. D **66**, 043503 (2002).
[18] R. Bernabei *et al.*, Phys. Lett. B **389**, 757 (1996); **408**, 439 (1997); **424**, 195 (1998); **450**, 448 (1999); **480**, 23 (2000).
[19] P. D. Sackett, *Galaxy Dynamics*, edited by D. Merritt, J. A. Sellwood, and M. Valluri, ASP Conf. Series, No. 182 (ASP, San Francisco, 1999), p. 393.
[20] R.P. Olling and M.R. Merrifield, Mon. Not. R. Astron. Soc. **311**, 361 (2000).
[21] R. Ibata, M. Irwin, G.F. Lewis, and A. Stolte, Astrophys. J. Lett. **547**, L133 (2001); R. Ibata, G.F. Lewis, M. Irwin, E. Totten, and T. Quinn, Astrophys. J. **551**, 294 (2001).
[22] M. Odenkirchen, P. Brosche, M. Geffert, and H.J. Tucholke, New Astron. **2**, 477 (1997).
[23] C. Power *et al.*, astro-ph/0201544.
[24] A. Tasitsiomi, astro-ph/0205464.
[25] J.S. Bullock, A.V. Kravtsov, and D. Weinberg, Astrophys. J. **539**, 517 (2000).
[26] E. Hayashi, J.F. Navarro, J.E. Taylor, J. Stadel, and T. Quinn, astro-ph/0203004.
[27] F. Stoehr, S.D.M. White, G. Tormen, and V. Springel, astro-ph/0203342.
[28] N. Katz and J.E. Gunn, Astrophys. J. **377**, 365 (1991); J. Dubinski, *ibid.* **431**, 617 (1994).
[29] T. Fukushige and M. Junichiro, Astrophys. J. **557**, 533 (2001).
[30] B. Moore, T. Quinn, F. Governato, J. Stadel, and G. Lake, Mon. Not. R. Astron. Soc. **310**, 1147 (1999).
[31] S.D.M. White and M. Rees, Mon. Not. R. Astron. Soc. **183**, 341 (1978); G.R. Blumenthal, S.M. Faber, J.R. Primack, and M.J. Rees, Nature (London) **311**, 517 (1984); M. Davis, G. Efstathiou, C.S. Frenk, and S.D.M. White, Astrophys. J. **292**, 517 (1985).
[32] J. Binney and S. Tremaine, *Galactic Dynamics* (Princeton University Press, Princeton, NJ, 1987).
[33] A. Helmi and S.D.M. White, Mon. Not. R. Astron. Soc. **307**, 495 (1999).
[34] S. Cole and C. Lacey, Mon. Not. R. Astron. Soc. **281**, 716 (1996); V.R. Eke, S. Cole, and C.S. Frenk, *ibid.* **282**, 263

(1996); G. Bryan and M. Norman, Astrophys. J. **321**, 80 (1998).
[35] J.R. Bond, S. Cole, G. Efstathiou, and N. Kaiser, Astrophys. J. **379**, 440 (1991); C. Lacey and S. Cole, Mon. Not. R. Astron. Soc. **262**, 627 (1993).
[36] S. Hofmann, D.J. Schwarz, and H. Stocker, Phys. Rev. D **64**, 083507 (2001).
[37] G. Jungman, M. Kamionkowski, and K. Griest, Phys. Rep. **267**, 195 (1996).
[38] L.P. Osipkov, Pis'ma Astron. Zh. **55**, 77 (1979); D. Merritt, Astron. J. **90**, 1027 (1985).
[39] J.F. Navarro, C.S. Frenk, and S.D.M. White, Astrophys. J. **462**, 563 (1996); **490**, 493 (1997).
[40] L.M. Widrow, Astrophys. J., Suppl. Ser. **131**, 39 (2000).
[41] J.D. Lewin and P.F. Smith, Astropart. Phys. **6**, 87 (1996).
[42] A.M. Green, Phys. Rev. D **65**, 023520 (2002).
[43] J.S. Bullock *et al.*, Mon. Not. R. Astron. Soc. **321**, 559 (2001).
[44] V.R. Eke, J.F. Navarro, and M. Steinmetz, Astrophys. J. **554**, 114 (2001).
[45] P. Ullio, L. Bergström, J. Edsjö, and C. Lacey, astro-ph/0207125.
[46] G. Duda, G. Gelmini, and P. Gondolo, Phys. Lett. B **529**, 187 (2002).